Intracellular drug delivery by poly(lactic-co-glycolic acid) nanoparticles, revisited

Peisheng Xu[1], **Emily Gullotti**[2], **Ling Tong**[2], **Christopher B. Highley**[3], **Divya R. Errabelli**[4], **Tayyaba Hasan**[4], **Ji-Xin Cheng**[2], **Daniel S. Kohane**[3,5], and **Yoon Yeo**[1,2,*]

1 *Department of Industrial and Physical Pharmacy, Purdue University, 575 Stadium Mall Drive, West Lafayette, IN 47907, USA*

2 *Weldon School of Biomedical Engineering, Purdue University, 206 South Martin Jischke Drive, West Lafayette, IN 47907, USA*

3 *Department of Chemical Engineering, 77 Massachusetts Avenue E25–342, Massachusetts Institute of Technology, Cambridge, MA 02139, USA*

4 *Wellman Center for Photomedicine, Harvard Medical School, Massachusetts General Hospital, 40 Blossom Street, Boston, MA 02114, USA*

5 *Laboratory for Biomaterials and Drug Delivery, Dept of Anesthesiology, Children's Hospital, Harvard Medical School, 300 Longwood Ave, Boston, MA 02115, USA*

Abstract

We reexamined the cellular drug delivery mechanism by poly(lactic-co-glycolic acid) nanoparticles (PLGA NPs) to determine their utility and limitations as an intracellular drug delivery system. First, we prepared PLGA NPs which physically encapsulated Nile red (a hydrophobic fluorescent dye), in accordance with the usual procedure for labeling PLGA NPs, incubated them with mesothelial cells, and observed an increase in the intracellular fluorescence. We then prepared NPs from PLGA chemically conjugated to a fluorescent dye and observed their uptake by the mesothelial cells using confocal microscopy. We also used Coherent Anti-Stokes Raman Scattering (CARS) microscopy to image cellular uptake of unlabeled PLGA NPs. Results of this study coherently suggest that PLGA NPs (i) are not readily taken up by cells, but (ii) deliver the payload to cells by extracellular drug release and/or direct drug transfer to contacting cells, which are contrasted with the prevalent view. From this alternative standpoint, we analyzed cytotoxicities of doxorubicin and paclitaxel delivered by PLGA NPs and compared with those of free drugs. Finally, we revisit previous findings in the literature and discuss potential strategies to achieve efficient drug delivery to the target tissues using PLGA NPs.

Keywords

PLGA nanoparticles; intracellular drug delivery; cellular uptake; contact-based transfer

---

* Corresponding author: Yoon Yeo, Ph.D. Phone: 765.496.9608 Fax: 765.494.6545 E-mail: yyeo@purdue.edu.

INTRODUCTION

Polymeric nanoparticles (NPs) have been widely explored for drug delivery. Advantages of NP systems are the small size, which makes them compatible with various administration routes including intravenous injection, and the relatively high drug encapsulation capacity (as compared to drug-polymer conjugates). Given that angiogenic tumors tend to develop permeable vasculature and can selectively recruit circulating small particles (enhanced permeability and retention effect; EPR effect),[1, 2] the small size of NPs is also useful for tumor-targeted drug delivery. Upon arrival at the target sites, NPs may release the drug outside the cells or enter the cells and unload the drug at the desired intracellular locations.[3] Small molecules that can easily traverse the cell membrane would work in either scenario. However, the following cases may require that the NPs be taken up by the cells: when the drug is unable to cross the cell membrane efficiently (*e.g.,* nucleic acids), a high level of a drug is needed in the intracellular location (*e.g.,* photodynamic therapy), or the drug is easily removed from the cells (*e.g.,* multidrug resistance).

Poly(lactic-co-glycolic acid) (PLGA) is a widely-used polymer for fabricating NPs because of biocompatibility, long-standing track record in biomedical applications, and well-documented utility for sustained drug release. Several studies have investigated the mechanism of intracellular drug delivery by PLGA NPs. It is generally thought that PLGA NPs are taken up by endocytosis and then release the drug at intracellular locations. Many studies demonstrated rapid and efficient cellular uptake of PLGA NPs, based on microscopic observation of PLGA NPs encapsulating a fluorescent probe and/or measurement of the intracellular level of the probe.[4-15] In contrast, an earlier study has argued that PLGA NPs transfer lipophilic markers to cell membrane, leading to an overestimation of cellular uptake of PLGA NPs.[16] In a related vein, another recent study demonstrated the transfer of lipophilic markers from polymeric micelles to a lipophilic environment,[17] challenging traditional understanding of micelle-based drug delivery.

The objectives of this study were to revisit the prevalent view of intracellular drug delivery by PLGA NPs in awareness of an alternative possibility and to determine the utility and limitations of PLGA NPs as an intracellular drug delivery system. Here we reexamined the cellular drug delivery mechanism by PLGA NPs in cell models comparable to those in existing studies, using confocal microscopy, flow cytometry, and Coherent Anti-Stokes Raman Scattering (CARS) microscopy.[18] First, we prepared PLGA NPs which physically encapsulated Nile red (a hydrophobic fluorescent dye) in accordance with the usual procedure for labeling PLGA NPs, incubated them with mesothelial cells, and observed an increase in the intracellular fluorescence. We then prepared NPs from a PLGA chemically conjugated to a fluorescent dye and observed their uptake by the mesothelial cells using confocal microscopy. We also used CARS microscopy to image cellular uptake of unlabeled PLGA NPs. Results of this study show that PLGA NPs (i) are not readily taken up by cells but (ii) deliver the payload to cells by extracellular drug release and/or direct drug transfer to contacting cells, which are contrasted with the prevalent view. Cytotoxicities of doxorubicin and paclitaxel delivered by PLGA NPs are compared with those of free drugs from this alternative standpoint.

EXPERIMENTAL SECTION

Materials

Poly (lactic-co-glycolic) acid (PLGA, lactide:glycolide = 65:35, Mw 118kDa, ester end group) was purchased from Lakeshore Biomaterials (Birmingham, AL), PLGA (lactide:glycolide = 50:50, carboxylate end group, inherent viscosity: 0.18 dL/g, Mw: 4000 Da) from Lactel absorbable polymers (Pelham, AL). Polyvinyl alcohol (Mw 6,000 Da) was purchased from Polysciences, Inc. (Warrington, PA, USA). Oregon Green-labeled paclitaxel, cell culture

media, and supplements were purchased from Invitrogen Corp. (Carlsbad, CA). Doxorubicin · HCl was purchased from Bidragon Pharmservice LLC (Burlingame, CA). Dipalmitoylphosphatidylcholine (DPPC) was purchased from Lipoid GmbH (Ludwigshafen, Germany). All other reagents were purchased from Sigma-Aldrich (St. Louis, MO).

Preparation and characterization of PLGA nanoparticles

PLGA NPs prepared for this study are summarized in Table 1. PLGA NPs physically encapsulating Nile red (NR/NP) were prepared using the single emulsion method. PLGA (118kDa) 200 mg and Nile red 2 mg were dissolved in 5 ml of dichloromethane or 3:2 mixture of dichloromethane and acetone. The polymer solution was directly added to 20 ml of 5% polyvinyl alcohol. The mixture was then homogenized for 30 seconds (for 300 nm particles: denoted as "NR/NP$_{300}$") or 10 min (for 100 nm particles: denoted as "NR/NP$_{100}$") using a probe sonicator (Vibracell VCX 400, Sonics & Materials Inc., Dunbury, CT) to generate an oil-in-water (o/w) emulsion. The formed emulsion was added to 100 ml distilled water and stirred for 1 hour at room temperature. After removing the remaining solvents by evaporation, the NPs were collected by centrifugation, and further purified by ultrafiltration (membrane MWCO: 500,000) or by multiple washing with distilled water. PLGA NPs physically encapsulating Oregon Green-labeled paclitaxel (OG-PTX/NP) and paclitaxel (PTX/NP) were prepared similarly. PLGA NPs physically encapsulating doxorubicin · HCl were prepared similarly, except that doxorubicin · HCl was first dissolved in water and then emulsified in the PLGA phase (i.e., double emulsion method) prior to homogenization in the PVA solution.

PLGA NPs chemically modified with a fluorescent dye (fl-NP) were prepared using PLGA conjugated to fluoresceinamine (FA-PLGA). FA-PLGA was prepared using the carbodiimide chemistry. Briefly, PLGA (4000 Da, with carboxylate end group, 4.0 g) was dissolved in 40 ml of dichloromethane, after that 560 mg of DCC (dicyclohexylcarbodiimide) and 311 mg NHS (N-hydroxysuccinimide) were added and stirred overnight at room temperature. Byproduct precipitates were removed by filtration. Fluoresceinamine/DMSO solution (0.0583 g FA in 20 ml DMSO) was then added to the filtrate and stirred overnight under the protection from light. The resulting product was precipitated in distilled water after removing dichloromethane. The polymer was purified by repeated dissolution in acetone and precipitation in ethanol, and then lyophilized. fl-NPs were prepared using a 3:1 mixture of PLGA (4000 Da) and FA-PLGA.

Size and surface charge of PLGA NPs were determined using a Zetasizer Nano-ZS90 (Malvern Instruments, Worcestershire, United Kingdom). Nile red content in NR/NP was determined by dissolving dry powders of a known weight in 2:1 mixture of dimethyl sulfoxide and acetone and measuring the Nile red absorbance at 550 nm. Doxorubicin content in Dox/NP was determined by measuring the doxorubicin absorbance at 486 nm using DMSO as a solvent. Paclitaxel content in PTX/NP was determined using HPLC (Column: Ascentis C18-column (25 cm×4.6 mm, particle size 5 μm); mobile phase: mixture of acetonitrile and water (50:50, v/v); flow rate: 1 ml/min; detection: 227 nm). Oregon green-paclitaxel in OG-PTX/NP was also determined by HPLC (Ascentis C18-column (25 cm×4.6 mm, particle size 5 μm); mobile phase: mixture of acetonitrile and water (linear gradient from 50:50 to 90:10, v/v, over 10 min); flow rate: 1 ml/min; detection: 227 nm).

Cell culture

Human mesothelial cells (CRL-9444, ATCC) were cultured in Medium 199 (Invitrogen), containing Earle's salts, L-glutamine, and 2.2 g/L sodium bicarbonate and supplemented with 3.3 nM epidermal growth factor, 400 nM hydrocortisone, 870 nM insulin, 20 mM HEPES, 10% fetal bovine serum (FBS), 100 U/ml penicillin, and 100 μg/ml streptomycin. OVCAR-5 ovarian cancer cell line (Fox Chase Cancer Institute, Philadelphia, PA) and KB human

nasopharyngeal carcinoma cell line (ATCC) were maintained in RPMI-1640, and MCF-7 human breast cancer cell line (ATCC) in DMEM; both media were supplemented with 10% fetal calf or bovine serum, 100 U/ml penicillin, and 100 μg/ml streptomycin. Cells were maintained at 37°C in a humidified atmosphere of 5% CO_2.

Confocal microscopy

For confocal microscopy of real-time uptake of NR/NPs, mesothelial cells were plated in 35 mm plates (11.8 cm^2) at a density of 100,000 cells in 3 ml of culture medium. After overnight, the culture medium was replaced with 2 ml of fresh medium containing NPs equivalent to 0.5 μM Nile red (The amount of NPs added to the medium was 0.01 − 0.1 mg/ml.). After 1 min, 30 min, and 180 min of incubation in the presence of particles, the medium was replaced with a particle-free fresh medium and immediately imaged with confocal laser scanning fluorescence microscopy (Leica TCS 4D scanner attached to a Leitz DMBR/E microscope, Leica, Deerfield, IL) operated by TCS-NT software (Leica, Deerfield, IL). An argon ion laser (488 nm) was used for excitation. The pinhole size was set to 0.3 μm throughout. The signal of Nile red fluorescence was detected using a long-pass filter (>590 nm) and displayed in red.

Cellular uptakes of fl-NPs, OG-PTX/NPs, and Dox/NPs were observed using an Olympus X81 confocal microscope. Mesothelial cells and MCF7 cells were plated in 35 mm glass bottom dishes (MatTek) at a density of 100,000 cells in 2 ml of culture medium. After overnight, the culture medium was replaced with 2 ml of fresh medium containing 0.1 mg/ml NPs. After 3 h of incubation in the presence of particles, the medium was replaced with a particle-free fresh medium and imaged with the Olympus X81 microscope operated with Fluoview software (Olympus, Japan). Fl-NPs were excited using a 488-nm laser, and its emission was read from 497 to 560 nm and expressed in green. OG-PTX/NPs were excited using a 488-nm laser, and its emission was read from 500 to 550 nm and expressed in green. The DOX/NPs were excited using a 488-nm laser, and its emission was read from 550 to 620 nm and expressed in red. Images were processed with NIH ImageJ.

Fluorescence Activated Cell Sorting (FACS)

Mesothelial cells were plated in a 6-well plate (9.6 cm^2) at a density of 500,000 cells per well. After overnight, the culture medium was replaced with 2 ml of fresh medium containing NPs equivalent to 0.5 μM Nile red. Fresh medium was used as a negative control. After 1 min, 30 min, and 180 min of incubation in the presence of particles, cells were washed with fresh medium twice, then with phosphate-buffered saline (PBS), and trypsinized for FACS analysis (FACScan flow cytometer, Becton Dickinson). Another set of cells were treated and washed in the same way, and then further incubated in the particle-free fresh medium for 180 min. In all FACS analysis, cell debris and free particles were excluded by setting a gate on the plot of side-scattered light (SSC) vs. forward-scattered light (FSC). A total of 30,000 gated cells were analyzed. The increase of fluorescence in the cells treated with NPs relative to that in the untreated control cells was expressed as:

Fluorescence increase relative to control = Log of red fluorescence intensity of cells incubated with particles / Log of red fluorescence intensity of untreated cells.

Quantitative analysis of Nile red uptake

Four sets of mesothelial cells were incubated with NR/NPs containing 0.5 μM Nile red for 180 min as described in *Confocal microscopy*. The cells were washed with fresh medium twice, then with PBS once, and incubated in the particle-free fresh medium for 0, 30, 60, and 180 min. At each time point, 2 ml of the medium was carefully sampled from one set of cells. The cells were permeabilized by freezing and thawing. Both permeabilized cells and recovered medium were lyophilized and suspended in a 2 ml 1:1 mixture of DMSO and water. Two ml

chloroform was then added to these suspensions to extract Nile red. One ml of chloroform was sampled, and the solvent was removed by evaporation. The dried samples were redissolved in DMSO and the amount of Nile red was analyzed using Tecan Spectrafluor Plus microplate reader (excitation/emission = 485 nm/595 nm). It was validated that this extraction method resulted in 91±3.5% recovery of Nile red from the NR/NPs in the medium. As a control, cells not incubated with NR/NPs were treated in the same way, and fluorescence intensities of the cells and medium were measured as background readings. The results were reported after subtracting the background readings from the fluorescence intensities of samples treated with the NR/NPs.

Release of fluorescence probe in the presence of serum protein or lipid

To determine the probe release prior to cellular uptake of NPs, the NPs were incubated in PBS, PBS with FBS, or PBS with liposomes. First, liposomes were prepared by the film hydration method. Briefly, 237 mg of DPPC was dissolved in 50 ml chloroform in a round-bottomed flask. Chloroform was evaporated under reduced pressure using a Yamato Rotary Evaporator at 40°C to form a thin lipid film. Fifty mL of PBS was added to hydrate the film, and the resulting suspension was sonicated for 2 hours in a Branson sonic bath. To remove residual chloroform, the liposome suspension was evaporated under reduced pressure in a 65°C water bath for 4 hours. The liposomes were filtered using a Stericup 0.22 μm filter and diluted with an additional 50 ml PBS, making the final concentration of liposomes in PBS 2.4 mg/ml.

Five mg of NR/NPs (283.7 ± 2.2 nm) or fl-NPs (300.4 ± 4.7 nm) were suspended in PBS, PBS with 10% FBS, or PBS with 2.4 mg/ml liposomes in a microcentrifuge tube and incubated with rotation at 37°C. After 1 hour, the tubes were spun for 5 minutes at 12,000 rpm. 0.8 ml of supernatant was collected and frozen. 0.8 ml of fresh release medium was added to each tube, which was sonicated for 10−20 minutes in a Branson sonic bath to resuspend the NP pellets. The NPs were further incubated at 37°C, and additional samples were taken at 3, 6, 12, and 24 hours. The samples were filtered using 0.2 μm syringe filter to ensure complete removal of NPs before analysis by Tecan microplate reader. The fluorescence of Nile red in the filtrated supernatant (released from NR/NP) was measured at excitation/emission wavelengths of 485 nm and 595 nm, and that of fluoresceinamine and/or FA-PLGA in the filtrated supernatant (released from fl-NP) was measured at excitation/emission wavelengths of 485 nm and 535 nm. Additionally, absorbance and fluorescence of PBS, PBS with 10% FBS, and PBS with liposomes were recorded as a background measurement.

To determine whether NR/NPs directly transfer the dye to liposomes based on contact or Nile red is released from NR/NPs to PBS first and then transferred to liposomes, the supernatant of NR/NP suspension in PBS was separated from NR/NPs and then incubated with liposomes. Briefly, NR/NPs were incubated in PBS for 3 hours at 37°C, and the supernatant was separated from NR/NPs by centrifugation (12,000 rpm, 5 min) and filtration (through 0.2 μm syringe filter). The supernatant were then incubated with liposomes for another 3 hours, and its fluorescence was compared with that of liposome solution that was incubated with an equal amount of NR/NPs for the same period.

Coherent Anti-Stokes Raman Scattering (CARS) microscopy

To observe the uptake of PLGA NPs without fluorescence labeling, CARS microscopy was performed. The setup of laser-scanning CARS microscopy has been presented in a previous report.[19] Pump and Stokes laser beams were generated by two tightly synchronized (Lok-to-Clock, Spectra-Physics, Mountain View, CA) Ti: sapphire oscillators with a pulse width of 5 ps (Tsunami, Spectra-Physics, Mountain View, CA). The two parallel-polarization beams were collinearly combined and directed into a laser-scanning confocal microscope (FV300/IX71, Olympus America, Center Valley, PA). The pump laser was tuned to 14140 cm^{-1} (ω_p) and the

Stokes laser was tuned to 11300 cm^{-1} or 11200 cm^{-1} (ω_s). A 60x water immersion objective (1.2 NA) was used to focus the excitation beams on the sample. The powers at sample for pump and Stokes lasers were 51 mW and 33 mW, respectively. Forward detected CARS signal was collected by an air condenser (0.55 NA) and detected with a photomultiplier tube (PMT, R3896, Hamamatsu, Japan). Bandpass filters (600/65 nm, Ealing Catalog, Rocklin, CA) were used to transmit the CARS signal. A hundred μl of 1 mg/ml unlabeled NPs (274.3 ± 7.8 nm) (i.e., 0.1 mg/ml NPs) were added to KB cells grown in 1 ml RPMI 1640 medium complemented with 10% FBS. CARS imaging was performed post 3-hour incubation with the NPs.

Cytotoxicity of Dox/NPs and PTX/NPs

Cytotoxicity of Dox/NPs and PTX/NPs were evaluated with MTT (3-(4,5-Dimethylthiazol-2-yl)-2,5-diphenyl-tetrazolium bromide) assay. MCF-7 human breast cancer cells were seeded in 96-well plates at an initial density of 8,000 cells per well in complete DMEM medium. After 24 hours of incubation, the medium was replaced with 200 μl of fresh medium containing PTX/NPs (equivalent to 1−1000 nM of paclitaxel) or Dox/NPs (equivalent to 0.05−10 μM of doxorubicin). Free (unencapsulated) paclitaxel or doxorubicin of equivalent concentrations was added in parallel for comparison. The MTT assay was performed after 48−72 hours of incubation with the drugs. The cell viability was quantified by measuring the UV absorbance at 560 nm with a Tecan microplate reader. The measured absorbance was normalized to the absorbance of non-treated control cells.

Another set of cytotoxicity test was performed to determine the contribution of drug release and/or contact-based drug transfer to the cytotoxic effect of PTX/NPs. We incubated one group of cells limiting their direct contact with the NPs and compared with the other group that was allowed to contact the NPs. For this purpose, Transwells® (pore size: 0.4 μm, the smallest pore size commercially available; Corning) was used in an anticipation that the Transwells® would reduce the contact between PTX/NPs and cells, although it may not completely prevent the PTX/NPs (269.3 nm) from going through the membrane. PTX/NPs (1−1000 nM) were added in the Transwells®, which were placed over the overnight grown MCF-7 cell layers. In another group of cells, PTX/NPs were placed beneath the Transwells®, allowing contact between PTX/NPs and cells. As a control, free paclitaxel of equivalent doses were added above or beneath the Transwells®, and their cytotoxic effects were compared to test if the Transwells® functions as a diffusion barrier of released paclitaxel. After 48 hours of incubation, cell viability was tested using the MTT assay.

In vitro release kinetics of PTX/NPs

The *in-vitro* drug release from PTX/NPs was monitored using dialysis. In brief, PTX/NPs equivalent to 30 μg of paclitaxel were suspended in 0.5 ml PBS and placed in a dialysis tube (MWCO: 10,000, Spectra/Por). The dialysis tube was placed in a receiving compartment filled with 9.5 ml DMEM complete medium (containing 10% FBS) and incubated at 37°C. At regular time intervals, 1 ml medium was sampled from the receiving compartment, and an equal volume of fresh medium was replaced. The sampled medium was stored at 4°C until analysis. For extraction of paclitaxel from the release medium, 4 ml of dichloromethane was added to 1 ml of the release medium, which was vortex-mixed for 30 seconds and centrifuged at 2000 g for 10 min. The organic phase was separated, dried with nitrogen, reconstituted in 1 ml of a 70:30 v/v mixture of methanol and water, and analyzed with HPLC (Column: Ascentis C18-column (25 cm×4.6 mm, particle size 5 μm); mobile phase: mixture of methanol and water (65:35, v/v), column temperature: 35°C; flow rate: 0.8 ml/min; detection: 230 nm). The extraction efficiency was 85.6%.

RESULTS

Incubation of cells with NR/NPs increased the intracellular fluorescence rapidly

PLGA NPs used in this study are summarized in Table 1. First, PLGA NPs physically encapsulating Nile red (NR/NPs) were prepared in two sizes (average size: 99.2 nm (NR/NP_{100}) and 311.0 nm (NR/NP_{300}); the subscript denotes mean diameter). At pH 7.4, both particles showed negative zeta potential (Table 1). Due to the high surface area to volume ratio, NR/NP_{100} showed much lower encapsulation efficiencies (encapsulated Nile red / theoretical Nile red: $9.9 \pm 0.2\%$) than NR/NP_{300} ($89.6 \pm 0.7\%$).

To observe uptake of NR/NPs, mesothelial cells were incubated in the presence of NR/NP_{100} or NR/NP_{300} for 1, 30, or 180 min and imaged with confocal microscopy immediately after replacing the particle suspension in the medium with fresh particle-free medium (Figure 1A). Irrespective of the particle size, red fluorescence was seen inside the cells, especially in the perinuclear region, as early as 1 min after incubation with the NR/NPs. Fluorescence intensity in the cells increased with incubation time. OVCAR-5 ovarian cancer cell line (Figure 1B) and KB human nasopharyngeal carcinoma cells (supplemental Figure 1) grown in the presence of NR/NP_{300} showed similarly rapid increase of red fluorescence in the cells. The microscopic observation was confirmed using a fluorescence activated cell sorter (FACS) (hatched bars in Figure 2). Consistent with the results of confocal microscopy, fluorescence was detected in the cells incubated with PLGA nanoparticles as early as 1 minute after incubation, and fluorescence intensity of the cells increased with the duration of incubation, according to the linear regression analysis ($p < 0.05$ for both NR/NPs).

Intracellular fluorescence decreased rapidly upon removal of NR/NPs

In the microscopic observation, we noted that red fluorescence started to appear outside of the cells, when particle-free fresh medium was added to replace the NR/NP_{300} suspension after >30 min incubation (Figure 1, marked in white circles). This could represent the NR/NPs detached from the cell surface or the efflux of Nile red from inside the cells. To determine the cause, we incubated the mesothelial cells with NR/NPs, washed them thoroughly, and maintained them in the particle-free medium for additional 3 hours. The fluorescence intensity of the cells (white bars in Figure 2) was measured with FACS and compared with that obtained immediately after the washing (hatched bars in Figure 2). Irrespective of particle size and duration of exposure, incubation in the particle-free medium resulted in significant decrease of cellular fluorescence. This result indicated that the fluorescence decrease was caused by efflux of Nile red from the cells rather than detachment of surface-bound NR/NPs. To further confirm this observation, intra- and extracellular dye levels were analyzed quantitatively. Mesothelial cells incubated with NR/NPs for 3 hours were thoroughly washed and maintained in the particle-free fresh medium, the cells and the medium were separately sampled over 180 min, and Nile red in the cells or the medium was analyzed. Nile red level in the cells started to decrease rapidly upon exposure to the particle-free medium (to 37% of original level for NR/NP_{100} and 54% for NR/NP_{300} in 30 min), and that in the medium increased simultaneously (Figure 3), indicating that intracellular Nile red was released into the particle-free medium over time.

In exploring the decrease of Nile red fluorescence in the cells we also considered other possibilities. It is unlikely that the decrease in fluorescence resulted from cell death, because both NR/NP_{100} and NR/NP_{300} were found to be non-toxic at the tested concentrations (0.01 or 0.1 mg/ml) (Supplemental Figure 2). It is also unlikely that the fluorescence decrease was due to the increase of the cell number (*i.e.*, decreased number of particles per cell), because our experiments were completed in 6 hours, and the average population-doubling times for most adherent continuous cell lines are 24−36 hours.[20] Moreover, fluorescence quenching is

excluded because fluorescence outputs of NR/NP$_{100}$ and NR/NP$_{300}$ remained stable over 3 hours at tested concentrations (Supplemental Figure 3A). Finally, we examined whether the decrease in fluorescence was due to the acidic pH of endosomal compartments,[21] in which NPs would have ended up if they had been endocytosed. The fluorescent intensity of NR/NPs incubated in the complete medium acidified with HCl to pH 4.8 did not significantly change over 3 hours (supplemental Figure 3B), indicating that the decrease was not caused by the acidic pH of the late endo-/ lysosomes. These results, as well as those of the microscopy, flow cytometry, and dye-extraction studies, suggest that the decrease in cellular fluorescence was caused by the efflux of Nile red from the cells.

NR/NPs release Nile red in the presence of serum or liposomes

Although NR/NP uptake was apparently consistent with the earlier studies,[4, 6, 9, 10, 12-14] the fact that both the increase and the decrease in the intracellular fluorescence signal occur rapidly led us to suspect that the fluorescence signal we have observed may not be the true representation of PLGA NPs. Given that Nile red is a lipophilic dye routinely used for staining intracellular lipid bodies,[22] it is possible that Nile red was released in the culture medium and then taken up by the cells or directly transferred to the membrane of contacting cells. To investigate this possibility, we incubated the NR/NP$_{300}$ (283.7 ± 2.2 nm) in phosphate-buffered saline (PBS, pH 7.4) containing hydrophobic or amphiphilic components that NR/NP$_{300}$ would encounter in the cell-culture medium. NR/NP$_{300}$ was incubated in PBS, PBS containing 10% fetal bovine serum (FBS/PBS), or PBS containing 2.4 mg/ml of liposomes (liposome/PBS). FBS was included to represent the amphiphilic components in the culture medium. Liposomes were used to mimic the lipid cellular membrane, although the contact between NR/NP$_{300}$ and the lipid membrane may be exaggerated in this model due to the small size (high surface area-to-volume ratio) of liposomes. These release buffers were separated from NR/NP$_{300}$ after timed incubation, and the Nile red fluorescence in each buffer solution was measured. As shown in Figure 4A, a moderate level of Nile red fluorescence was detected in FBS/PBS. Much stronger Nile red fluorescence was detected in liposome/PBS as early as in 1 hour and significantly increased after 3 hours. On the other hand, Nile red fluorescence was negligible in PBS, which indicated lack of Nile red release in PBS in the absence of FBS or liposomes. However, we could not completely exclude an alternative possibility that Nile red was first released but not detected, because fluorescence of Nile red in aqueous environment is very weak.[23] To determine whether Nile red is directly transferred from NR/NP$_{300}$ to liposomes or serum proteins via contact or released from NR/NP$_{300}$ in PBS first and then picked up by them, NR/NP$_{300}$ were incubated in PBS first, and the supernatant was separated from NR/NP$_{300}$ and then incubated with liposomes. No fluorescence was detected in the liposome solution, which confirmed that Nile red release in PBS was indeed negligible. To evaluate the Nile red release relative to the total encapsulated dye, the release experiment was repeated with NR/NP$_{100}$ and NR/NP$_{300}$ in the same media for 3 hours, and the released Nile red was extracted to chloroform and subjected to the HPLC analysis (Supplemental Methods). Since we noted in the previous experiment that a significant fraction of aggregated proteins and liposomes were excluded during filtration, which was performed to ensure complete removal of NR/NPs from the release medium, the extraction was performed without filtration (therefore, the difference in relative Nile red signals between Figure 4 and Supplemental Figure 4B would be explained by the exclusion of aggregated proteins and liposomes in the former). As shown in the Supplemental Figure 4A, NR/NP$_{100}$ showed a modest release of Nile red in PBS but ~50% (in the first hour) and additional ~25% (in 1−3 hours) of Nile red in FBS/PBS or liposome/PBS. The % Nile red from NR/NP$_{300}$ was relatively lower than NR/NP$_{100}$ in all three media, which would be explained by the lower surface-area to volume ratio. Nile red release from NR/NP$_{300}$ was negligible in PBS (Supplemental Figure 4B), consistent with the fluorescence readings (Figure 4). In FBS/PBS and liposome/PBS, NR/NP$_{300}$ released 16.4 and 25% in 3 hours, respectively. The two release experiments consistently show that Nile red is released to the media in the

presence of hydrophobic or amphiphilic components, which are prevalent in the cell culture condition. This result suggests that NR/NPs in the culture medium are likely to release Nile red to the medium and/or transfer to the membrane of contacting cells directly. Therefore, the fluorescence signal seen in the cells (Figures 1-3) should not be interpreted as the level of NR/ NP uptake.

Confocal imaging of chemically labeled NPs and CARS microscopy showed that PLGA NPs were not readily taken up by the cells

Since Nile red could be separated from NR/NPs and transferred to hydrophobic or amphiphilic components, we prepared *chemically* labeled NPs (fl-NPs) using PLGA conjugated to fluoresceinamine (FA-PLGA; Figure 5A) to keep track of the polymer itself. When fl-NPs (300.4 ± 4.7 nm) were exposed to PBS, FBS/PBS, and liposome/PBS, the chemically-conjugated fluorescence probe could not be freed from the NPs as easily as Nile red. Unlike NR/NPs, fluorescence from fl-NPs gradually increased over 24 hours, most likely due to the release of fluresceinamine itself or FA-PLGA conjugate, more in FBS/PBS than in liposome/ PBS. Fluorescence increase in the first 3 hours of incubation (the time frame in which incubation and confocal microscopy were typically performed) corresponded to 2.7−8.5% of total encapsulated fluoresceinamine (Supplemental Figure 4C). The fluorescence increase at the later time points (12, 24 hours) could be attributed to the release of FA-PLGA following the initial polymer degradation, which occurs relatively quickly in PLGA used for fl-NPs (LA/ GA=50/50, 4000 Da).[24, 25]

Having learned that fluorescence release from fl-NPs in FBS/PBS and liposome/PBS would not be as significant as that from NR/NPs during the initial 3 hours in the medium, we incubated fl-NPs (159.5 nm) with mesothelial cells and MCF-7 cells (human breast cancer cell line) in the same manner as NR/NPs and imaged them by confocal microscopy. In sharp contrast to NR/NPs, few fl-NPs were detected inside the cells after 3 hours of incubation for both cell lines (Figures 5B and 5C). We note that fl-NPs were made of a PLGA with carboxylate end groups for conjugation of fluoresceinamine; thus, the fl-NPs may not be directly comparable to NR/NPs, which were made of a PLGA with a high molecular weight and ester end groups. Although we did not observe any difference in the surface charge between fl-NPs and the other NPs made of PLGA with ester end groups (Table 1)--probably because of the residual PVA on the NP surface,[4] it is possible that the fl-NPs would have COOH groups on the surface, which may encourage the NPs to interact with cell surface glycocalyx through hydrogen bonding. It is, therefore, even more intriguing that fl-NPs were rarely observed in the cells despite the potential contribution of the COOH groups to the interaction with cells.

To confirm the lack of NP uptake observed by confocal microscopy with fl-NPs, Coherent Anti-Stokes Raman Scattering (CARS)[18] microscopy was utilized. The CARS spectra of PLGA film and intracellular lipid bodies in the C-H stretch vibration region are shown in Figure 6A. PLGA exhibits a peak at 2940 cm^{-1} arising from the CH_3 stretch vibration and the lipid bodies show a peak at 2840 cm^{-1} arising from the CH_2 stretch vibration in the aliphatic carbon chains. This difference allowed us to distinguish the PLGA NPs from intracellular lipid bodies without labeling them. KB cells were incubated with PLGA NPs (274.3 nm) for 3 hours and imaged by CARS. The lipid bodies (bright contrast in the 2840 cm^{-1} image, Figure 6B) were seen inside the cells. In contrast, the PLGA NPs (visible in the 2940 cm^{-1} image but not in the 2840 cm^{-1}) were only found in the extracellular space, but not in the KB cells (Figure 6C). For parallel comparison, confocal microscopy and CARS were performed on the same KB cells incubated with NR/NP$_{300}$ for 3 hours (Supplemental Figure 5). The red intracellular signals observed in confocal microscopy were co-localized with lipid bodies (2840 cm^{-1}), whereas the extracellular signals were seen as PLGA (2940 cm^{-1}: Note that the extracellular signals do not exactly co-localize because the extracellular NPs were in constant motion.). The

CARS observation also supports that PLGA NPs were not readily taken up by cells, at least in 3 hours.

Despite the lack of cellular uptake, NPs delivered the physically encapsulated drugs to the cells – an indication of contact-based transfer and/or uptake of released drugs

Confocal microscopy with fl-NPs, CARS, and Nile red release experiments collectively indicate that the fluorescence increase in the cells incubated with NR/NPs is mainly a result of Nile red transfer from NR/NPs to the cells rather than uptake of the NPs. We then investigated if PLGA NPs encapsulating other drug molecules would deliver the drugs to the cells in a similar manner, and how this would influence bioactivity of the drugs. We prepared PLGA NPs physically encapsulating doxorubicin (Dox/NP, 254.1 nm, doxorubicin content: $0.23 \pm 0.01\%$w/w), paclitaxel (PTX/NP, 269.3 nm, paclitaxel content: $2.03 \pm 0.2\%$w/w), or Oregon green-paclitaxel (OG-PTX/NP, 228.8 nm) and performed confocal microscopy and cytotoxicity test. When MCF-7 cells were incubated with OG-PTX/NPs or Dox/NPs for 3 hours, Oregon green-paclitaxel (Figure 7A) and doxorubicin (Figure 7B) were readily observed in the cells, similarly to the results observed with NR/NPs (Figure 1, Supplemental Figure 1A).

Fluorescent signals of Oregon green-paclitaxel were seen in the cytosol, and the intensity was comparable to that of free drugs (Figure 7A). In contrast, doxorubicin was observed mostly in the nuclei, and the intensity appeared to be much weaker in the cells incubated with Dox/NPs than that with free doxorubicin (Figure 7B). We hypothesized that Dox/NPs and OG-PTX/NPs compared differently with their free drug counterparts in the intracellular fluorescence intensity because of the difference in hydrophobicities of doxorubicin and paclitaxel. In the lack of cellular uptake of NPs, potential mechanisms by which paclitaxel or doxorubicin in PLGA NPs is transferred to the cells would be extracellular drug release followed by uptake and/or contact-based drug transfer to the cells. If the drug is released first and then taken up, the level of drug in the cells incubated with drug/NPs would be lower than that with free drug of equivalent dose. On the other hand, if drug/NPs directly transfer the drug to cells, the drug/NPs may serve as a supply of concentrated drug molecules; thus, even a higher level of drug than that in free drug solution would potentially be achieved in the cells. Therefore, one explanation for the relatively weak doxorubicin intensity obtained with Dox/NPs (Figure 7B) would be that doxorubicin favored the former mechanism (release from Dox/NPs followed by uptake), whereas paclitaxel, which is more hydrophobic than doxorubicin,[26] would have been directly transferred from the NPs, at least in part, resulting in comparable drug signal to that of free drug solution. In an attempt to validate this explanation, the drug uptake was evaluated by comparing dose response curves of PTX/NPs (1−1000 nM) and Dox/NPs (0.05−10 μM) in MCF-7 breast cancer cells with those of free drugs of equivalent doses. Given the difference in fluorescence intensity, one may expect that cytotoxicity of free doxorubicin would be greater than that of Dox/NPs. However, we were unable to detect any significant difference in dose response curves of Dox/NPs and free doxorubicin (Supplemental Figure 6A), which would be mainly attributed to the instability of free doxorubicin in cell-culture medium ($t_{1/2}$ of 920 μM doxorubicin solution at 37°C: 5 hours[27]). Cytotoxicity of PTX/NPs was comparable to that of free paclitaxel (Supplemental Figure 6B), consistent with the microscopic observation. Given that free paclitaxel is stable in aqueous medium ($t_{1/2}$ at 43°C: 149 years[28]) unlike doxorubicin, the fact that PTX/NPs showed comparable cytotoxicity to that of free doxorubicin indicates that cellular delivery of paclitaxel by PTX/NPs could, at least partly, be attributed to contact-based drug transfer to the cells.

Cytotoxicity of PTX/NPs is attributed to uptake of released paclitaxel and contact-based transfer

To examine the contribution of drug release and/or contact-based drug transfer to the cytotoxic effect of PTX/NPs, MCF-7 cells were incubated with PTX/NPs while reducing contact between

the two using Transwells® (Corning; pore size: 0.4 μm, the smallest pore size commercially available) (Supplemental Figure 7A). The PTX/NPs, be they placed above or beneath the Transwells®, showed comparable cytotoxicity to that of free paclitaxel counterpart (Supplemental Figure 7B). The fact that PTX/NPs placed above the Transwells® (PTX/NPs with limited contact with cells) had cytotoxic effect indicates that paclitaxel release from PTX/NPs was substantial. Given the high affinity of paclitaxel to albumin,[29] the paclitaxel release might have been facilitated by the presence of serum proteins in the culture medium. The PTX/NPs with limited contact with cells were less toxic than those allowed to contact cells, especially at 10 nM (t-test; p < 0.01). However, this alone would not prove the contribution of direct contact between PTX/NPs with cells, because the control experiment performed with free paclitaxel indicated that the Transwells® itself could function as a diffusion barrier to the free drug, probably due to the drug adsorption to the membrane (free PTX-reduced contact vs. free PTX-full contact: p < 0.05 at 1 nM and 1000 nM).

Therefore, *in-vitro* paclitaxel release from PTX/NPs was examined in the complete cell culture medium. PTX/NPs equivalent to 30 μg of paclitaxel was dispersed in 0.5 ml PBS, put in a dialysis bag (MWCO: 10,000), and placed in 9.5 ml DMEM supplemented with 10% FBS, making the total paclitaxel concentration in the system 3 μg/ml. Since the reported solubility of amorphous paclitaxel in water at 37°C was as high as 3.5 μg/ml[30] or 30 μg/ml,[31] it was assumed that the paclitaxel release would not be limited by the aqueous solubility. As shown in Figure 8, 5.8 ± 1.1% of the total paclitaxel was released in 30 min followed by additional 8% release in the next 3.5 hours. The cumulative paclitaxel release in 24 hours was 15.7 ± 1.4%, which was comparable to the value reported in the literature.[15] We note that PTX/NP was first dispersed in PBS and contained in a dialysis bag for easy separation from the release medium (DMEM with 10% FBS). This release model ensured that the released paclitaxel (MW: 853) could freely traverse the dialysis membrane (MWCO: 10,000) and bind the serum proteins in the receiving compartment, but it did not allow for direct contact between PTX/NPs and serum proteins, which might have resulted in a higher percentage of released paclitaxel. Despite the limitation of this release model, the result shows that the paclitaxel release from the PTX/NPs was slow and limited. This suggests that the cytotoxicity of PTX/NPs, which was comparable to that of free paclitaxel, would not be entirely due to the paclitaxel release but also depended on the contact-based transfer.

DISCUSSION

We examined the mechanism of intracellular drug delivery by PLGA NPs and proposed an alternative view. While previous studies have reported efficient intracellular uptake of PLGA NPs based on fluorescence microscopy and physically-encapsulated probes, our work using confocal microscopy and a chemically-conjugated probe as well as CARS microscopy and unlabeled NPs shows that the NP uptake does not occur as efficiently as previously reported. Intracellular fluorescence increase that we and others have observed with physically-encapsulated probes appears to be a result of dye transfer rather than NP uptake. From this perspective, some of previous findings can be interpreted alternatively. First, Sahoo *et al.* reported that residual PVA on the NP surface prevented cellular 'uptake' of the particles, represented by intracellular level of 6-coumarin, a hydrophobic fluorescence probe.[4] This result was attributed to the increased hydrophilicity of the particle surface. Our alternative interpretation is that the surface PVA might have prevented direct contact between cells and the NPs, limiting the contact-based transfer of 6-coumarin. Second, previous studies found that the efficiency of PLGA NP uptake increased as the particle size decreased.[9, 12, 14] While this size dependence may be viewed as evidence of endocytosis[9] (and small NPs (<100 nm) may do enter the cells relatively easily than the NPs discussed here), it is also possible that the higher intracellular fluorescence resulted from the higher surface area to volume ratio of the smaller particles, which would increase the area of contact with the cells. Third, Chavanpatil *et al.*

reported that PLGA NPs delivering paclitaxel was not effective in the multidrug resistant tumor cells.[32] The authors explain that the PLGA NPs are taken up by the cells, but the released paclitaxel is rapidly effluxed by P-glycoprotein. Our alternative view is that PLGA NPs did not enter the cells in the first place but rather delivered drugs via release or contact-based transfer. Although originally encapsulated in PLGA NPs, the paclitaxel would have been introduced to the cells as a free drug, subjected to the P-glycoprotein efflux just as efficiently as free paclitaxel.

In this study, the release- or contact-mediated transfer of the physically encapsulated payloads to the cells was demonstrated using small molecular-weight and hydrophobic molecules, such as Nile red or paclitaxel. Relatively more hydrophilic doxorubicin · HCl also appears to be transferred to the cells (Figure 7B), but it remains to be seen whether the other hydrophilic and/ or larger molecules are taken up by the cells in a similar manner. In the context of small molecular weight hydrophobic drugs at least, the results of this study warrant the following recommendations for future development of PLGA NP systems as an intracellular drug delivery system. First, leaching-out of the payload from PLGA NPs during their systemic circulation should be minimized. Our release study shows that PLGA NPs released a moderate amount of Nile red in the presence of serum proteins. This indicates that the PLGA NPs in the current form will not completely prevent drug release in circulation. Given that tumor-selective accumulation of NPs (EPR effect) is predicated on prolonged circulation of NPs, preventing drug release from NPs on the way to target tissues would be critical in utilizing the PLGA NPs for tumor-targeted drug delivery. Second, surface modification of PLGA NPs would be needed to promote their cellular uptake upon arrival at the target tissues. A number of studies have focused on improving cellular recognition[33-36] and uptake,[37] but such surface modifications may make the NP systems more susceptible to nonspecific immune clearance. In this regard, it is worthwhile to note a recent attempt to achieve both prolonged circulation and efficient cellular uptake by programming the NPs to change the surface property at the target tissues.[38]

Finally, an important message from this work is that data from studies of cellular uptake and intracellular trafficking of NPs using fluorescent probes should be interpreted with greater caution. In the beginning of this study, we used Nile red, a lipophilic fluorescent dye. However, comparison of confocal microscopy of NR/NPs (physically encapsulating Nile red) and fl-NPs (fluoresceinamine chemically conjugated to the polymer) or CARS, which can image non-labeled NPs, has revealed that the actual cellular uptake of NPs is much less than that suggested by the confocal microscopy. In many studies, the use of physically-encapsulated probes as markers for NPs is justified by the fact that the probe is not released in a buffered saline (e.g., PBS). However, our release experiment shows that the fluorescent probe can be separated from the NPs and transferred to a lipid bilayer or serum proteins. In this context, a recent study using Förster resonance energy transfer imaging is noteworthy, as it demonstrated that polymeric micelles, although structurally different, were also not taken up by the cells as an intact form, but transferred the payload to the contacting cell membrane.[17] Physically-encapsulated fluorescent probes, even if they are seen in the cells, should not be considered as a representative of the NPs or any other types of nanocarriers.

Supplementary Material

Refer to Web version on PubMed Central for supplementary material.

ACKNOWLEDGMENT

REFERENCES

1. Matsumura Y, Maeda H. A New Concept for Macromolecular Therapeutics in Cancer Chemotherapy: Mechanism of Tumoritropic Accumulation of Proteins and the Antitumor Agent Smancs. Cancer Res 1986;46:6387–6392. [PubMed: 2946403]

2. Maeda H, Wu J, Sawa T, Matsumura Y, Hori K. Tumor vascular permeability and the EPR effect in macromolecular therapeutics: a review. Journal of Controlled Release 2000;65(1−2):271. [PubMed: 10699287]

3. Romberg B, Hennink W, Storm G. Sheddable Coatings for Long-Circulating Nanoparticles. Pharmaceutical research 2008;25(1):55–71. [PubMed: 17551809]

4. Sahoo SK, Panyam J, Prabha S, Labhasetwar V. Residual polyvinyl alcohol associated with poly(D,L-lactide-co-glycolide) nanoparticles affects their physical properties and cellular uptake. J. Controlled Release 2002;82:105–114.

5. Panyam J, Zhou W.-z. Prabha S, Sahoo SK, Labhasetwar V. Rapid endo-lysosomal escape of poly (DL-lactide-co-glycolide) nanoparticles: implications for drug and gene delivery. The FASEB Journal 2002;16:1217–1226. [PubMed: 12153989]

6. Panyam J, Sahoo SK, Prabha S, Bargar T, Labhasetwar V. Fluorescence and electron microscopy probes for cellular and tissue uptake of poly(d,l-lactide-co-glycolide) nanoparticles. International Journal of Pharmaceutics 2003;262(1−2):1–11. [PubMed: 12927382]

7. Prabha S, Labhasetwar V. Critical determinants in PLGA/PLA nanoparticle-mediated gene expression. Pharm. Res 2004;21(2):354–364. [PubMed: 15032319]

8. Panyam J, Labhasetwar V. Dynamics of endocytosis and exocytosis of poly(D,L-lactide-coglycolide) nanoparticles in vascular smooth muscle cells. Pharmaceutical research 2003;20(2):212–20. [PubMed: 12636159]

9. Desai MP, Labhasetwar V, Walter E, Levy RJ, Amidon GL. The mechanism of uptake of biodegradable microparticles in Caco-2 cells is size dependent. Pharm Res 1997;14(11):1568–1573. [PubMed: 9434276]

10. Win KY, Feng S-S. Effects of particle size and surface coating on cellular uptake of polymeric nanoparticles for oral delivery of anticancer drugs. Biomaterials 2005;26(15):2713–2722. [PubMed: 15585275]

11. Yoo HS, Park TG. Biodegradable nanoparticles containing protein-fatty acid complexes for oral delivery of salmon calcitonin. Journal of pharmaceutical sciences 2004;93(2):488–495. [PubMed: 14705204]

12. Qaddoumi MG, Ueda H, Yang J, Davda J, Labhasetwar V, Lee VHL. The characteristics and mechanisms of uptake of PLGA nanoparticles in rabbit conjunctival epithelial cell layers. Pharmaceutical research 2004;21(4):641–648. [PubMed: 15139521]

13. Cegnar M, Premzl A, Zavasnik-Bergant V, Kristl J, Kos J. Poly(lactide-co-glycolide) nanoparticles as a carrier system for delivering cysteine protease inhibitor cystatin into tumor cells. Experimental Cell Research 2004;301(2):223–231. [PubMed: 15530858]

14. Gvili K, Benny O, Danino D, Machluf M. Poly(D,L-lactide-co-glycolide acid) nanoparticles for DNA delivery: Waiving preparation complexity and increasing efficiency. Biopolymers 2007;85(5−6): 379–391. [PubMed: 17266128]

15. Vicari L, Musumeci T, Giannone I, Adamo L, Conticello C, De Maria R, Pignatello R, Puglisi G, Gulisano M. Paclitaxel loading in PLGA nanospheres affected the in vitro drug cell accumulation and antiproliferative activity. BMC Cancer 2008;8(1):212. [PubMed: 18657273]

16. Pietzonka P, Rothen-Rutishauser B, Langguth P, Wunderli-Allenspach H, Walter E, Merkle HP. Transfer of Lipophilic Markers from PLGA and Polystyrene Nanoparticles to Caco-2 Monolayers Mimics Particle Uptake. Pharmaceutical Research 2002;19(5):595. [PubMed: 12069160]

17. Chen H, Kim S, Li L, Wang S, Park K, Cheng J-X. Release of hydrophobic molecules from polymer micelles into cell membranes revealed by Forster resonance energy transfer imaging. Proceedings of the National Academy of Sciences 2008:6596–6601.

18. Cheng J-X. Coherent Anti-Stokes Raman Scattering Microscopy. Applied Spectroscopy 2007;91:197–208. [PubMed: 17910784]

19. Wang HW, Le TT, Cheng JX. Label-free imaging of arterial cells and extracellular matrix using a multimodal CARS microscope. Opt. Comm 2008;281:1813–1822.

20. Freshney, RI. Culture of Animal Cells. Wiley-Liss; New York: 2000.

21. Haag R, Kratz F. Polymer Therapeutics: Concepts and Applications. Angewandte Chemie International Edition 2006;45(8):1198–1215.

22. Greenspan P, Mayer EP, Fowler SD. Nile red: a selective fluorescent stain for intracellular lipid droplets. J. Cell Biol 1985;100(3):965–973. [PubMed: 3972906]

23. Ferrer ML, Monte F. d. Enhanced emission of Nile Red flourescent nanoparticles embedded in hybrid sol-gel glasses. J. Phys. Chem. B 2005;109:80–86. [PubMed: 16850987]

24. Park TG. Degradation of poly(lactic-co-glycolic acid) microspheres: effect of copolymer composition. Biomaterials 1995;16(15):1123–1130. [PubMed: 8562787]

25. http://www.lakeshorebio.com/products-stock-polymers.html

26. Song D, Wientjes MG, Au JLS. Bladder tissue pharmacokinetics of intravesical taxol. Cancer Chemotherapy and Pharmacology 1997;40(4):285–292. [PubMed: 9225946]

27. Janssen MJH, Crommelin DJA, Storm G, Hulshoff A. Doxorubicin decomposition on storage. Effect of pH, type of buffer and liposome encapsulation. International journal of pharmaceutics 1985;23 (1):1–11.

28. MacEachern-Keith GJ, Wagner Butterfield LJ, Incorvia Mattina MJ. Paclitaxel Stability in Solution. Anal. Chem 1997;69(1):72–77.

29. Paál K, Müller J, Hegedûs L. High affinity binding of paclitaxel to human serum albumin. European Journal of Biochemistry 2001;268(7):2187–2191. [PubMed: 11277943]

30. Liggins RT, Hunter WL, Burt HM. Solid-state characterization of paclitaxel. Journal of pharmaceutical sciences 1997;86(12):1458–1463. [PubMed: 9423162]

31. Swindell CS, Krauss NE, Horwitz SB, Ringel I. Biologically active taxol analogs with deleted A-ring side chain substituents and variable C-2′ configurations. J. Med. Chem 1991;34(3):1176–1184. [PubMed: 1672157]

32. Chavanpatil MD, Patil Y, Panyam J. Susceptibility of nanoparticle-encapsulated paclitaxel to P-glycoprotein-mediated drug efflux. International journal of pharmaceutics 2006;320(1−2):150–156. [PubMed: 16713148]

33. Kim SH, Jeong JH, Chun KW, Park TG. Target-Specific Cellular Uptake of PLGA Nanoparticles Coated with Poly(L-lysine)-Poly(ethylene glycol)-Folate Conjugate. Langmuir 2005;21(19):8852–8857. [PubMed: 16142970]

34. Farokhzad OC, Jon S, Khademhosseini A, Tran T-NT, LaVan DA, Langer R. Nanoparticle-aptamer bioconjugates: a new approach for targeting prostate cancer cells. Cancer Research 2004;64:7668–7672. [PubMed: 15520166]

35. Farokhzad OC, Cheng J, Teply BA, Sherifi I, Jon S, Kantoff PW, Richie JP, Langer R. Targeted nanoparticle-aptamer bioconjugates for cancer chemotherapy in vivo. Proc. Nat. Acad. Sci. USA 2006;103:6315–6320. [PubMed: 16606824]

36. Kocbek P, Obermajer N, Cegnar M, Kos J, Kristl J. Targeting cancer cells using PLGA nanoparticles surface modified with monoclonal antibody. Journal Of Controlled Release 2007;120(1−2):18–26. [PubMed: 17509712]

37. Mo Y, Lim L-Y. Paclitaxel-loaded PLGA nanoparticles: Potentiation of anticancer activity by surface conjugation with wheat germ agglutinin. Journal of Controlled Release 2005;108(2−3):244. [PubMed: 16213056]

38. Hatakeyama H, Akita H, Kogure K, Oishi M, Nagasaki Y, Kihira Y, Ueno M, Kobayashi H, Kikuchi H, Harashima H. Development of a novel systemic gene delivery system for cancer therapy with a tumor-specific cleavable PEG-lipid. Gene Therapy 2007;14(1):68–77. [PubMed: 16915290]
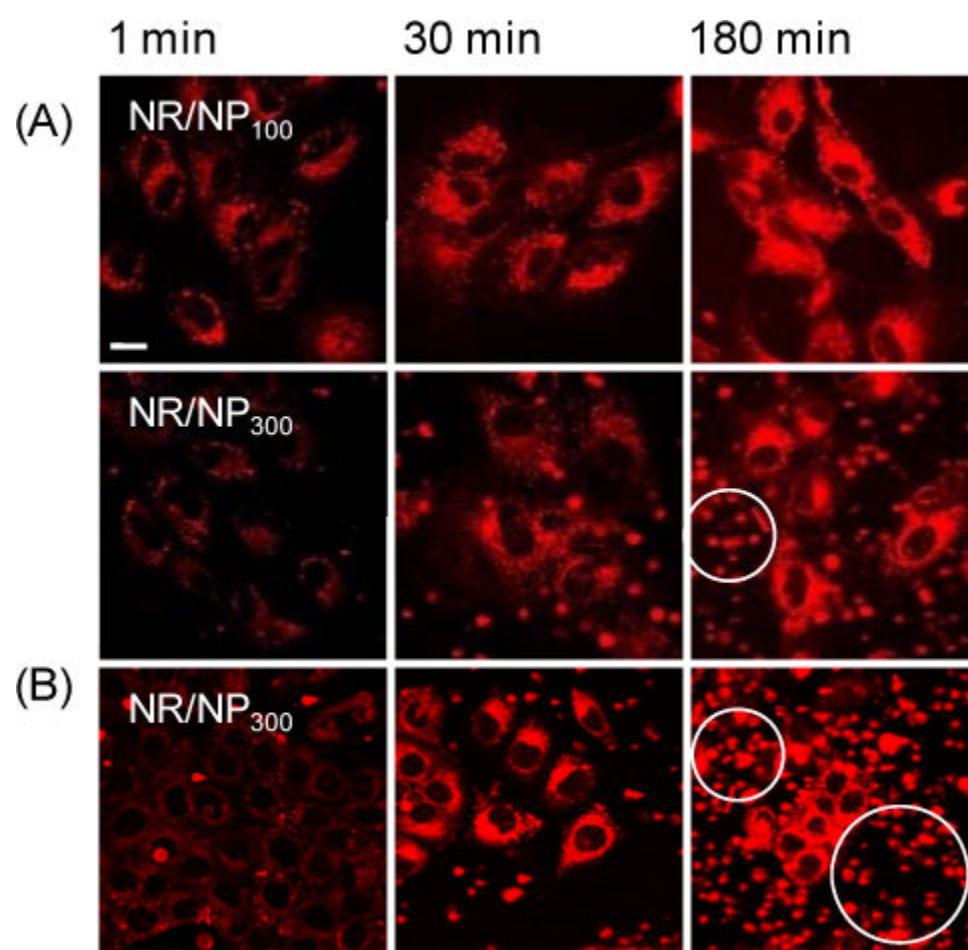
Figure 1.
Real time confocal microscopic images through the middle of (A) mesothelial cells and (B) OVCAR-5 cells incubated with NR/NPs. Cells were incubated with particles for the indicated times, and then were placed in the particle-free medium. Marked areas indicate red fluorescence that appeared outside of cells when particle-free fresh medium was added to replace the NR/ NP_{300} suspension. Scale bar = 20 μm.
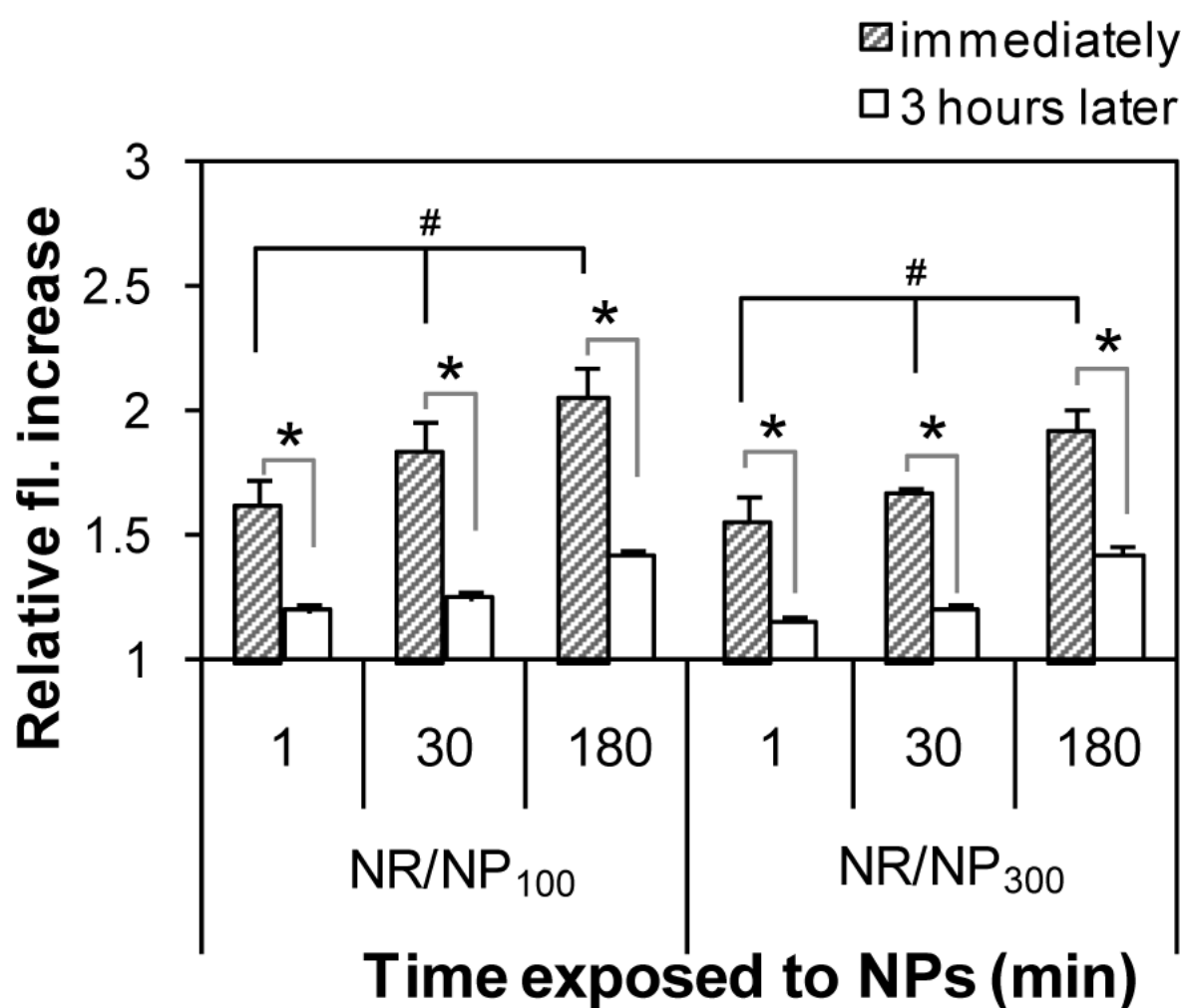
Figure 2.
FACS analysis of Nile red uptake by mesothelial cells. The cells were incubated with nanoparticles for 1, 30, or 180 min at 37°C and washed with fresh medium three times prior to FACS analysis. Values are log of red fluorescence intensity of cells incubated with NPs divided by log of red fluorescence intensity of untreated cells, reported as averages and standard deviations (n = 4). * and # indicate statistical difference (p < 0.05) based on the t-test and ANOVA test, respectively.
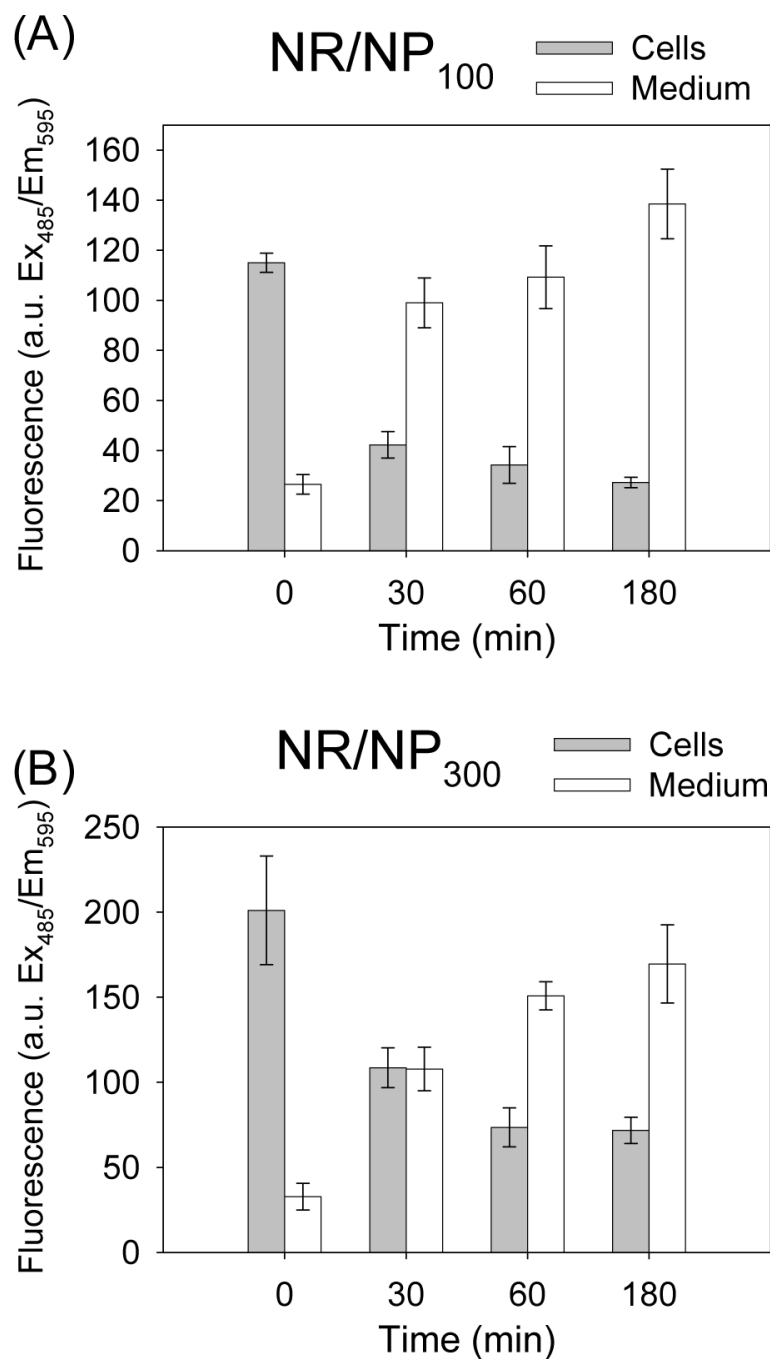
Figure 3.
Fluorescence changes in cells and in the medium during incubation in the particle-free medium. Mesothelial cells were incubated in the presence of NR/NP_{100} or NR/NP_{300} for 3 hours, washed with fresh medium twice and PBS once, and then incubated in particle-free fresh medium. Cells were separated from the medium after 0 min (i.e., immediately after washing), 30 min, 60 min, and 180 min in the particle-free medium. Cells were permeabilized by thawing and freezing. Nile red was extracted from permeabilized cells and cell-free medium. Values were reported as averages and standard deviations (n=4). In all cases, values at 30, 60, and 180 min were significantly different from the values at time 0 of corresponding samples (cells or medium) ($p < 0.01$).
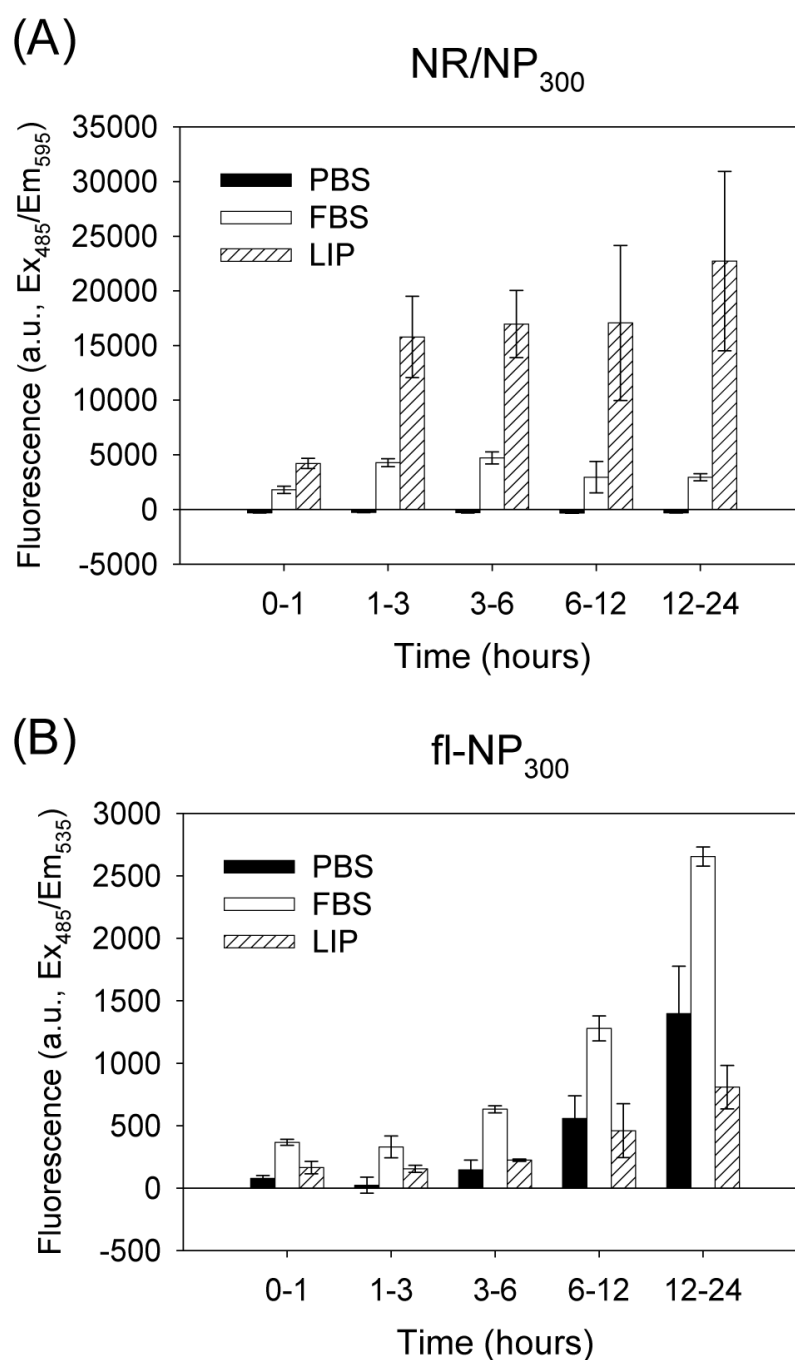
Figure 4.
Release of fluorescence probe in the presence of serum proteins or liposomes during the interval: (A) Nile red fluorescence released from NR/NPs and (B) fluoresceinamine fluorescence released from fl-NPs. Values were reported as averages and standard deviations (n=3). PBS: PBS only; FBS: 10% FBS in PBS (FBS/PBS); LIP: 2.4 mg/ml liposomes in PBS (liposome/PBS).
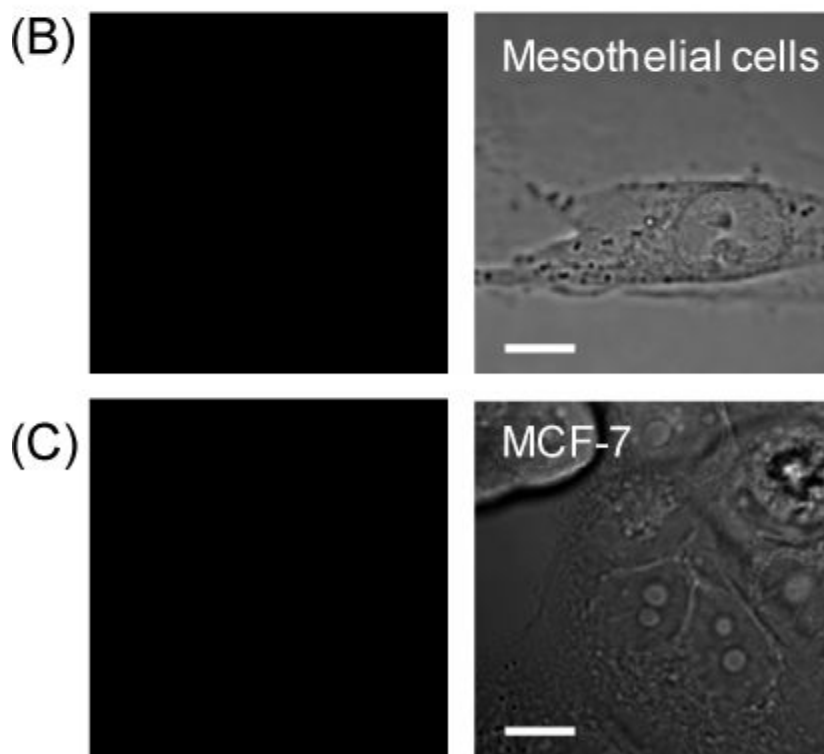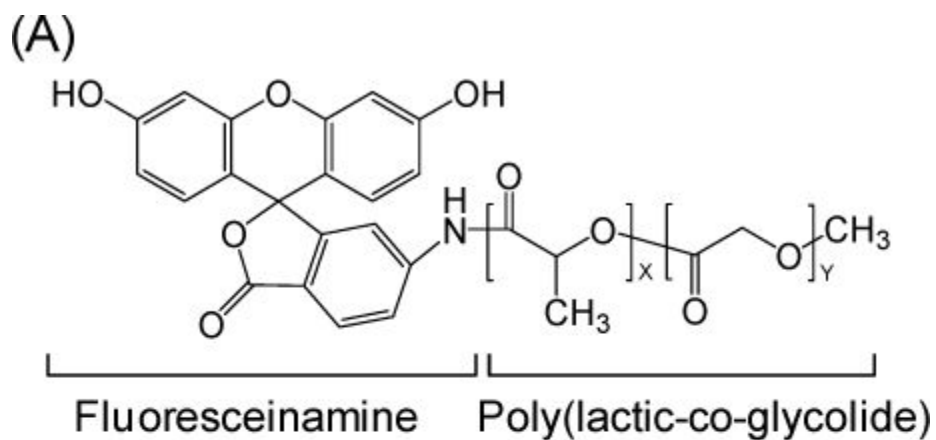
Figure 5.
(A) PLGA conjugated to fluoresceinamine (FA-PLGA); Confocal microscopic image showing absence of fl-NP uptake in 3 hours by (B) mesothelial cells and (C) MCF-7 cells. In B and C, images on the left show green channels (i.e., no nanoparticles); those on the right show transmission channels of the same field. Scale bars = 10 μm.
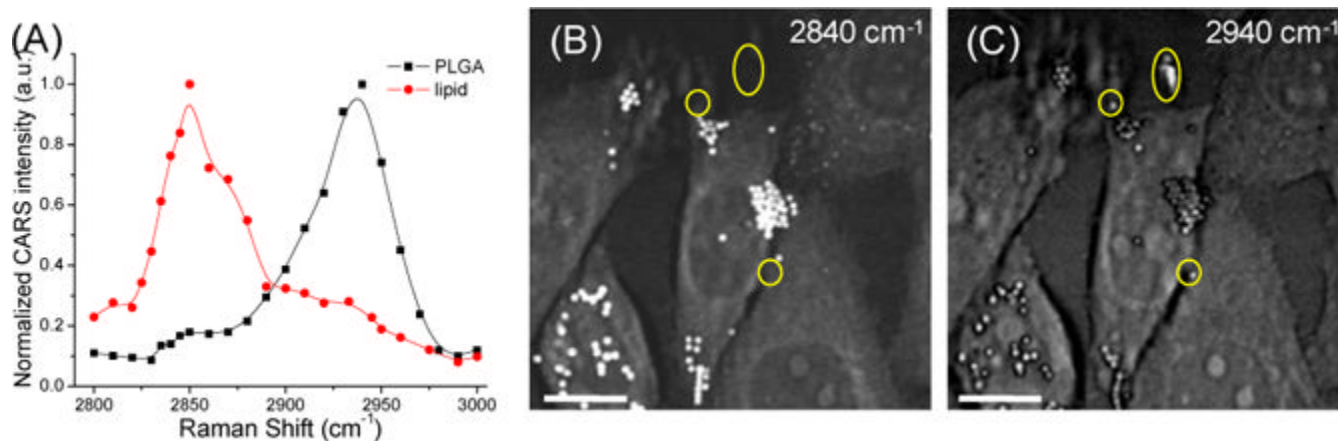
Figure 6.
Chemically selective imaging of intracellular lipid bodies and extracellular PLGA particles by CARS microscopy. (A) CARS spectra of a PLGA film and lipid bodies in KB cells. The two peaks at 2940 cm^{-1} and 2840 cm^{-1} arise from CH$_3$ stretch vibration in PLGA and CH$_2$ symmetric stretch vibration in lipid bodies, respectively. (B) CARS image with (ω_p- ω_s) at 2840 cm^{-1}. (C) CARS image with (ω_p- ω_s) at 2940 cm^{-1}. KB cells were incubated with unlabeled PLGA NPs for 3 hours. The CARS signals were detected in the forward direction. The lipid bodies produced a stronger signal at 2840 cm^{-1}, whereas the PLGA particles (in yellow circles) could only be seen at 2940 cm^{-1}. These data show that PLGA NPs did not enter KB cells after 3 hours of incubation with NPs. Scale bars = 10 μm.
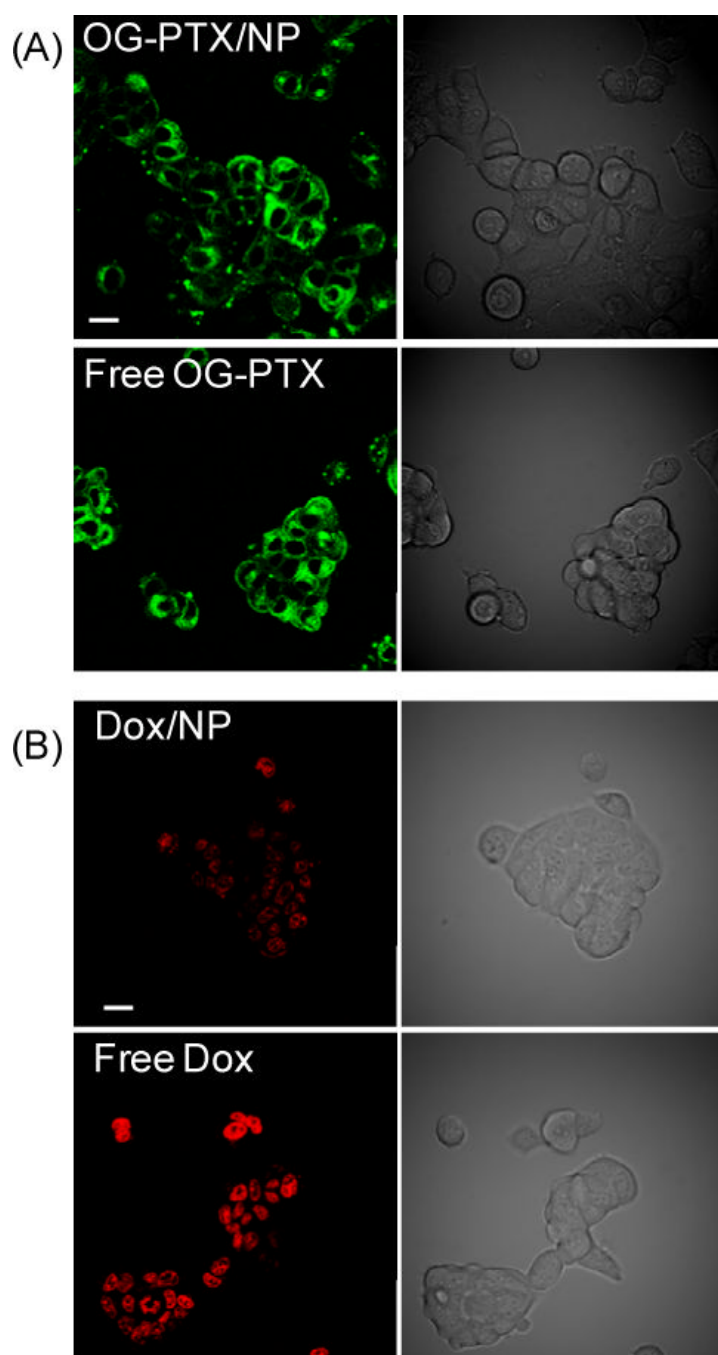
Figure 7.
Confocal microscopic images showing (A) Oregon red-paclitaxel uptake in MCF-7 cells incubated with OG-PTX/NPs (upper panel) or free Oregon red-paclitaxel solution (lower panel). Both treatments provided 584 nM Oregon green-paclitaxel.; (B) Doxorubicin uptake in MCF-7 cells incubated with Dox/NPs (upper panel) or free doxorubicin solution (lower panel). Both treatments provided 1.97 μM doxorubicin. Images on the left show green (Oregon green-paclitaxel) or red (doxorubicin) channels; those on the right show transmission channels.
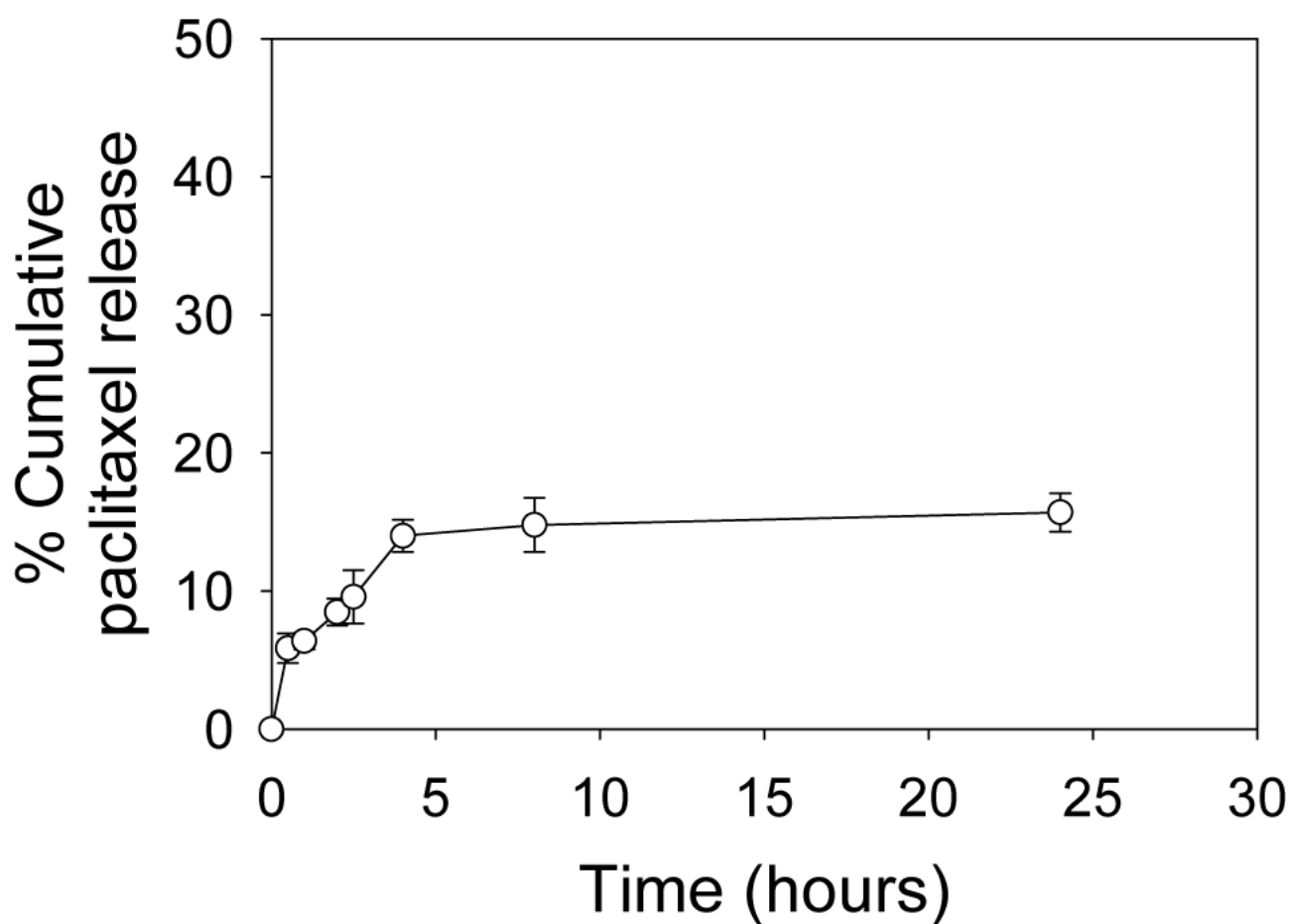
Figure 8.
In-vitro release kinetics of PTX/NPs. PTX/NPs equivalent to 30 μg of paclitaxel was suspended in 0.5 ml PBS, contained in a dialysis bag (MWCO: 10,000), and incubated in 9.5 ml DMEM supplemented with 10% FBS. The DMEM was sampled at regular time intervals, extracted with dichloromethane, and analyzed with HPLC. Values were reported as averages and standard deviations (n=3).

Table 1

PLGA NPs used in the experiment

Code[a]	PLGA	Particle size (nm)[b]	Zeta potential (mV)[c]	Fluorescent probe or active ingredient	Methods used to observe cellular uptake of NPs
NR/NP$_{100}$[d] or NR/NP$_{300}$[d]	LA/GA = 65/35 (118 kDa)	99.2 ± 0.9 311.0 ± 2.9	−1.24 ± 0.32 −0.62 ± 0.14	Nile red *physically* encapsulated in NP	Confocal microscopy; Flow cytometry; Fluorescent probe release
Fl-NP	LA/GA = 50/50 (4000 Da, carboxylate end group)	159.5 ± 2.8	−3.18 ± 0.22	Fluoresceinamine *chemically* conjugated to PLGA	Confocal microscopy
NP	LA/GA = 65/35 (118 kDa)	274.3 ± 7.8	−2.08 ± 0.49	None	CARS
Dox/NP	LA/GA = 65/35 (118 kDa)	254.1 ± 8.3	−3.11 ± 0.82	Doxorubicin · HCl *physically* encapsulated in NP	Confocal microscopy; MTT assay
OG-PTX/NP	LA/GA = 65/35 (118 kDa)	228.8 ± 3.5	−3.17 ± 0.19	Oregon Green-paclitaxel *physically* encapsulated in NP	Confocal microscopy
PTX/NP	LA/GA = 65/35 (118 kDa)	269.3 ± 1.0	−3.17 ± 0.09	Paclitaxel *physically* encapsulated in NP	MTT assay

[a] NP code: / indicates physical encapsulation: For example, NR/NP means NP physically encapsulating Nile red; - indicates chemical conjugate: For example, Fl-NP means NPs made of PLGA chemically conjugated to fluoresceinamine.

[b] Data represent average ± standard deviation (n = 3)

[c] Measured after adjusting pH to 7 with HCl: particle concentration 0.5 mg/ml

[d] The subscripts denote median diameter